Available online at www.sciencedirect.com
SCIENCE DIRECT
Polymer 47 (2006) 5538–5543
polymer
www.elsevier.com/locate/polymer

# Time dependent light attenuation measurements used in studies of the kinetics of polymer crystallization

B. Heck, T. Kawai, G. Strobl *

*Physikalisches Institut, Albert-Ludwigs-Universität, 79104 Freiburg, Germany*

Received 12 January 2005; received in revised form 9 November 2005; accepted 15 November 2005
Available online 11 May 2006

**Abstract**

Results obtained for different samples of s-polypropylene and poly (ethylene-*co*-octene) demonstrated the usefulness of light attenuation measurements in investigations of polymer crystallization. The earlier stages with separated growing spherulites fall in the range of Rayleigh–Debye–Gans scattering. Known relationships describing the dependence of the linear attenuation coefficient on the radius and the index of refraction of the spherulite can be applied in evaluations. The sensitivity of attenuation measurements is higher than that of conventional tools.


*Keywords:* Polymer crystallization; Spherulites; Light scattering

## 1. Introduction

Investigations of the kinetics of polymer crystallization are usually carried out by differential calorimetry, X-ray scattering in the wide- and small-angle range, dilatometry or time dependent vibrational spectroscopy. Although based on different properties there is not much difference in the sensitivity of all these methods. Reliable data are only obtained from values of the crystallinity in the range of some percent of the final values. This means that for growing spherulites, which usually reach end sizes in the order of several micrometers, measurements start only at sizes of several hundred nanometers. This, however, is already far away from the initial stages.

Presently, in discussions of the basic mechanism of polymer crystallization, these early stages have gained particular importance. There are good reasons to assume a crystal nucleation and growth which includes an intermediate phase, but the details, i.e., the natures and the sequence of transient phases have not yet been clarified. Different views are put forward. Some authors propose a preceding coverage of the whole volume by a mesomorphic phase which develops by a mechanism resembling a spinodal process [1,2], there exist clear indications for a nucleation into a mesomorphic phase [3], and we favor a picture with a mesomorphic phase in the front of a growing spherulite [4].

To discriminate between the different views, an experimental tool is required which follows the crystallization process with a sensitivity superior to the conventional methods. We found that measurements of the attenuation coefficient of light have this potential. During the last years we investigated polymer crystallization also with time dependent light scattering [5]. The sensitivity of this technique is limited by the restricted angular range of the usually employed CCD detectors and the intensity fluctuations of the laser light source. In addition, multiple scattering cannot be neglected over a larger part of the period of crystallization. Light attenuation measurements avoid these problems:

- the decrease in the transmission is due to photons scattered in all directions
- whether a photon is scattered once or several times is irrelevant
- the transmitted intensity can, in principle, be easily corrected for the fluctuation of the laser light source.

On the other hand, a problem may arise from photons which are scattered in forward direction and then cannot be separated from the primary beam. Light attenuation ('turbidity') measurements have already been applied in crystallization studies, but only in a few cases rather long ago [6–9], being at this time used for qualitative purposes only. By introducing known theoretical relationships for the total light scattering cross-section, we have now put the evaluation on a solid basis.

* Corresponding author.
*E-mail address:* strobl@uni-freiburg.de (G. Strobl).

0032-3861/$ - see front matter © 2006 Elsevier Ltd. All rights reserved.
doi:10.1016/j.polymer.2005.11.098

In the following, we report results obtained for different samples of syndiotactic polypropylene and poly (ethylene-*co*-octene). The results are compared to crystallization isotherms measured in the dilatometer and by small angle X-ray scattering, and the agreement shows that measurements of the light attenuation during the crystallization of a polymer can indeed be quite helpful.

## 2. Theoretical background

The attenuation of light after a passage through a plate-like sample with thickness $D$ is described by the Lambert–Beer law

$$\frac{I}{I_0} = \exp - \Lambda D. \tag{1}$$

$I_0$ denotes the flux of the light beam at the sample front, and $I$ gives the flux remaining after the beam has passed through the sample. The parameter $\Lambda$ is the linear attenuation coefficient. In general, the attenuation can be due to both, scattering and absorption of light, but the latter factor is absent for common polymers. In our experiments on crystallizing polymers, measurements were conducted for samples cooled from the melt to the crystallization temperature. At the beginning, they are still in the molten state but spherulites or hedrites are nucleated and grow successively. The contribution of the growing spherulites or hedrites to the linear attenuation coefficient $\Lambda$ follows from the change in the intensity, as

$$\Lambda = \frac{1}{D} \ln \frac{I(0)}{I(t)}. \tag{2}$$

As long as the scattering objects are diluted in the matrix, which is always the case during the initial stages of the crystallization process, $\Lambda$ is given by

$$\Lambda = \rho \sigma^2. \tag{3}$$

Here, $\rho$ describes the number density of objects and $\sigma^2$ is the total scattering cross-section. $\sigma^2$ is usually represented as

$$\sigma^2 = \pi R^2 Q, \tag{4}$$

where $Q$ represents a 'scattering efficiency factor'. Expressions for $Q$ are given in the literature, and one distinguishes between three different ranges, addressed as

- Rayleigh scattering
- Rayleigh–Debye–Gans scattering
- Mie scattering.

Explicit expressions exist for spherical scatterers. Here, the scattering cross-section depends on the radius $R$ of the sphere and the indices of refraction $n_m$, $n_s$ of the melt and the scattering object. The parameters included in the equations are the ratio of the indices of refraction

$$m = \frac{n_s}{n_m} \tag{5}$$

and a parameter $\alpha$ which is proportional to the radius

$$\alpha = \frac{2\pi n_m R}{\lambda_v}. \tag{6}$$

Here, $\lambda_v$ denotes the vacuum wavelength. Rayleigh scattering is found for $\alpha \ll 1$. The scattering efficiency factor here is given by [10]

$$Q_R = \frac{8}{3}\alpha^4 \left(\frac{m^2-1}{m^2+2}\right)^2. \tag{7}$$

In the next range, that of Rayleigh–Debye–Gans scattering, the scattering efficiency factor reads [11]

$$Q_{RDG} = (m-1)^2 \left[\frac{5}{2} + 2\alpha^2 - \frac{\sin(4\alpha)}{4\alpha} + \frac{7}{16\alpha^2}(1-\cos(4\alpha)) + \left(\frac{1}{2\alpha^2} - 2\right)(0.577 + \ln(4\alpha) + Ci(4\alpha))\right] \tag{8}$$

with

$$Ci(x) = -\int_x^\infty \frac{\cos x'}{x'} dx'. \tag{9}$$

Eq. (8) includes Eq. (7) as a limiting case for $\alpha \ll 1$. The full equations to be used in the case of Mie scattering are rather involved, but there exists an approximate expression. It follows for the 'anomalous diffraction model' and has the form [12]

$$Q_M \approx 2 - \frac{4}{\alpha'} \sin \alpha' + \frac{4}{(\alpha')^2}(1 - \cos \alpha'), \tag{10}$$

where $\alpha'$ is the modified variable

$$\alpha' = 2(m-1)\alpha. \tag{11}$$

Fig. 1 shows as an example results of a calculation of $\sigma^2$ carried out for the case of a crystallizing polyethylene, setting $n_m = 1.49$ and assuming for $n_s$ the relation

$$n_s = n_m + \phi_s(n_c - n_m), \tag{12}$$

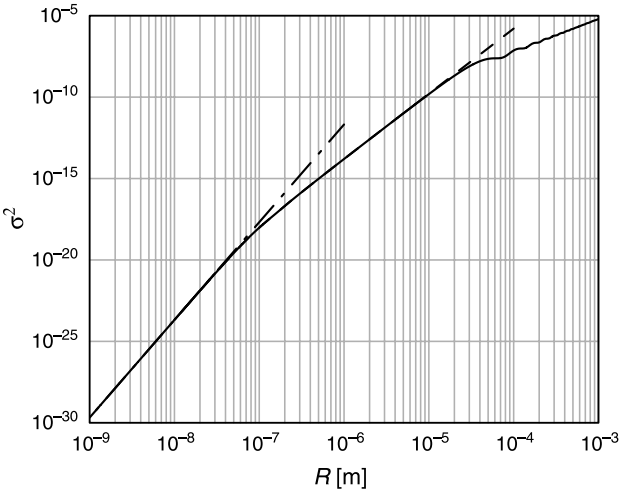


Fig. 1. Variation of the light scattering cross-section $\sigma^2$ of a sphere with the radius $R$. Calculation for the case of spherulites of PE with an inner crystallinity of 10% ($n_m = 1.54$, $n_c = 1.49$).

with $n_c = 1.54$; $\phi_s$ here describes the crystallinity within the spherulite. Calculations were carried out for $\phi_s = 0.1$. One can identify in the figure the three different ranges. The continuous curve was obtained by a combination of Eqs. (7), (8), (10) and includes the Rayleigh, the Rayleigh–Debye–Gans and the Mie region. The parts drawn with broken lines follow from applying Eqs. (7) and (8) exclusively. The three ranges differ in the dependence of the scattering cross-section $\sigma^2$ on the object radius $R$. One finds in the Rayleigh range

$$\sigma_R^2 \sim (m-1)^2 R^6, \tag{13}$$

in the Rayleigh–Debye–Gans range

$$\sigma_{RDG}^2 \sim (m-1)^2 R^4, \tag{14}$$

and in the Mie range

$$\sigma_M^2 \sim (m-1)^2 R^2. \tag{15}$$

The transitions between the three ranges are rather sharp and located around 100 nm and 10 μm. Experiments usually deal with objects in the central Rayleigh–Debye–Gans range where $\sigma^2 \sim (m-1)^2 R^4$.

As was already emphasized, these equations hold as long as the objects are isolated in the matrix. Application of the equations ends, when the objects touch each other. In fact, the attenuation factor then passes over a maximum and decreases again until homogeneity is reached when the sample is fully occupied by objects. Light attenuation then still exists due to the birefringence within the spherulites, but the main scattering following from the density difference between the melt and the spherulites has disappeared.

## 3. Experimental

In the determination of the attenuation factor we used the same set-up as for time dependent light scattering experiments, composed of a He–Ne laser, a sample holder with temperature control and a CCD-camera with 769×512 pixels on an area of 6.9×4.2 mm$^2$. The transmission coefficient $I/I_0$ was obtained by a restriction of the integration area to a circular region which just caught the primary beam. Time dependent data where stored in a PC for further evaluations. Details of the set-up have already been given [5].

Samples with a thickness in the order of 100 μm kept between two glass slides were put into a hot stage. Cooling from the melt to the preset crystallization temperature $T_c$ was usually achieved within 1–2 min.

The first results reported here were obtained for two commercial syndiotactic polypropylenes produced by Fina Co. (sPP-F) and Mitsui Co. (sPP-M). After an isothermal crystallization at elevated temperatures both had comparable crystallinities in the order of 0.30. According to the data sheet, the Fina product has 83% syndiotactic pentades and the Mitsui product 92% syndiotactic dyades. As a second example, measurements on two samples of poly(ethylene-*co*-octene), P(EcO14)D1, P(EcO14)D2, will be presented. They were supplied by Dow Co., and they have both an octene weight content of 14%.

The time dependent attenuation measurements are compared to the results of dilatometric measurements of the change of the specific volume and to a determination of the time dependence of the crystalline–amorphous interface area by small angle X-ray scattering (SAXS). We used a mercury-filled dilatometer and a Kratky-SAXS camera, employing standard methods for the data evaluation [13].

## 4. Results

In a previous work we measured with the dilatometer crystallization isotherms of the Fina sPP, and Fig. 2 reproduces some results [14]. The slope in the log–log plot indicates for the initial stages of the crystallization process a decrease of the specific volume proportional to $t^3$. An increase in the crystallization temperature just results in a parallel shift of the curves to longer times. Such a behavior is expected if the growing object—hedrites or spherulites—increases in size with a constant growth rate, i.e., for

$$R \sim t. \tag{16}$$

One therefore expects for the time dependence of the linear attenuation coefficient $\Lambda$ the law Eq. (15)

$$\Lambda \sim R^4 \sim t^4. \tag{17}$$

Fig. 3 demonstrates that this is indeed found. The slope in the log–log plots indicates an exponent of 4 during the initial stages. In the further development $\Lambda$ passes over a maximum and then decays to a final value. The time dependence during this later stage comes as qualitatively expected and is known since long time [6]. As was emphasized and demonstrated by Keane and Stein also in an early work [7], $\Lambda$ can be associated with the scattering intensity integrated over the full angular range from 0 to 180°. The latter reaches a maximum when the spherulites cover about half of the sample volume. The non-vanishing final value in the end state, where the sample is completely filled with spherulites is due to the orientation

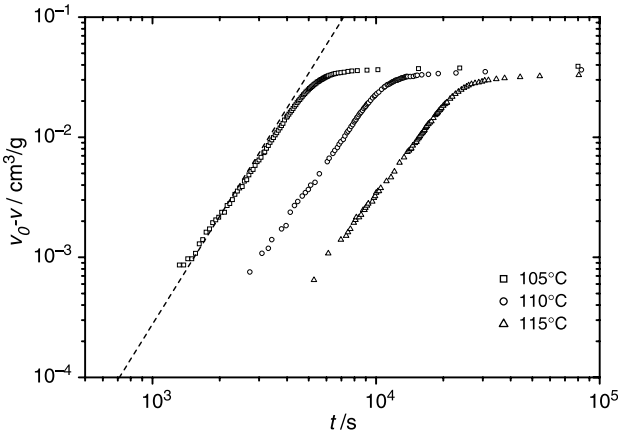


Fig. 2. sPP-F, dilatometric measurements: Change of the specific volume during isothermal crystallizations at the indicated temperatures. Slopes in the log–log plots indicate an initial decrease proportional to $t^3$ (from [14]).

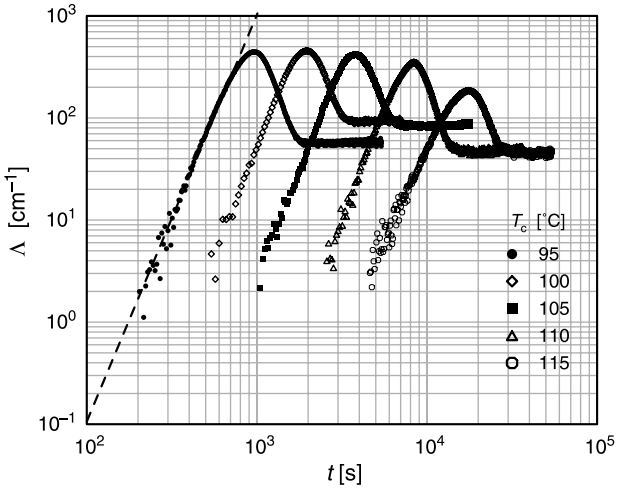


Fig. 3. sPP-F: change of the linear attenuation coefficient $\Lambda$ during isothermal crystallizations at the indicated temperatures. Initial slopes in the log–log plots indicate an initial increase proportional to $t^4$.

fluctuations of the optical indicatrix, whose direction in the spherulites varies with the orientation of the crystallized chains. Even if there is a basic understanding of the $\Lambda$-isotherms in the later stages we made no attempt here to quantitatively evaluate this part of the curve; our interests concerned first of all the initial stages of the crystallization process.

The other sPP sample, supplied by Mitsui Co., has a different crystallization behavior due to the addition of a nucleating agent in high concentration. This is demonstrated first by dilatometry. Fig. 4 indicates for the decrease of the specific volume $v$ during the initial stages of the crystallization process a power law

$$v_0 - v(t) \sim t^{4.5}, \tag{18}$$

where $v_o$ denotes the initial value. Generally, in the usual case of a constant number of growing objects, the decrease in the specific volume is given by

$$v_0 - v(t) \sim R^3(\Delta v), \tag{19}$$

where $\Delta v$ describes the specific volume difference between the growing object and the melt. If the growth is again linear,

$$R \sim t, \tag{20}$$

the observed exponent indicates an increasing inner order of the growing object according to

$$\Delta v \sim t^{1.5}. \tag{21}$$

Insertion processes, i.e., a growth of subsidiary lamellae in between two already existing dominant lamellae [15], can result in such an increase. For the linear attenuation coefficient we then expect

$$\Lambda \sim R^4(\Delta n)^2, \tag{22}$$

and therefore a time dependence

$$\Lambda \sim t^7. \tag{23}$$

Fig. 5 showing the results of time dependent transmission measurements, again carried out for different crystallization temperatures, demonstrates that the expectation is fulfilled. The increase of $\Lambda$ is proportional to the seventh power of the time.

The next two examples deal with the crystallization kinetics of P(EcO). Fig. 6 shows the time dependence of $\Lambda$ for the crystallization of the first sample, P(EcO14)D1. It obeys during the initial stages the power law

$$\Lambda \sim t^4, \tag{24}$$

indicative for a linear growth and a constant inner structure of the growing spherulites. The result is in agreement with a SAXS measurement. We derived from the scattering curves the Porod coefficient

$$P \sim O_{ac}(\Delta\eta_{ac})^2. \tag{25}$$

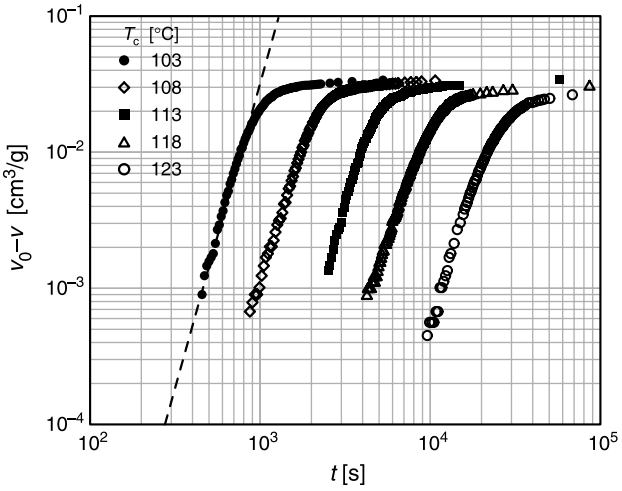


Fig. 4. sPP-M, dilatometric measurements: Change of the specific volume during isothermal crystallizations at the indicated temperatures. Initial slopes in the log–log plots indicate an initial decrease $v_0 - v \sim t^{4.5}$.

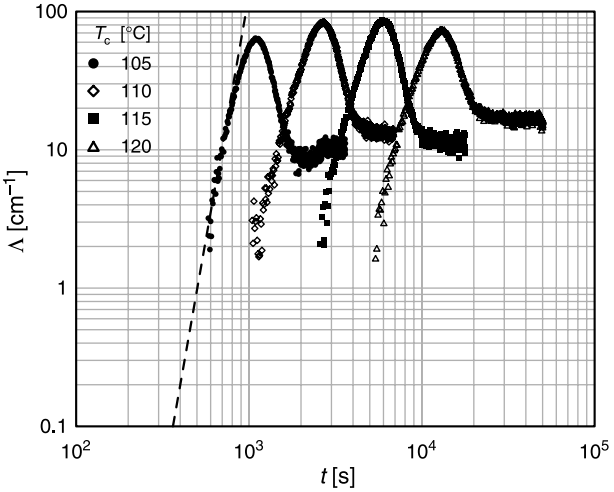


Fig. 5. sPP-M: change of the linear attenuation coefficient $\Lambda$ during isothermal crystallizations at the indicated temperatures. Initial slopes in the log–log plots indicate an initial increase proportional to $t^7$.

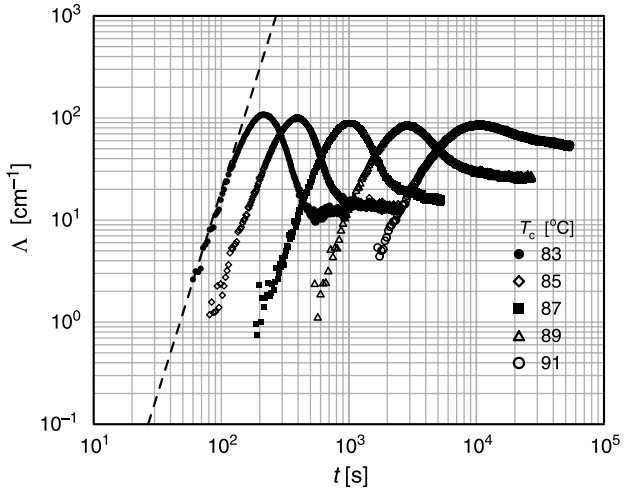


Fig. 6. P(PcoO14)D1: change of the linear attenuation coefficient $\Lambda$ during isothermal crystallizations at the indicated temperatures. Initial slopes in the log–log plots indicate an initial increase proportional to $t^4$.

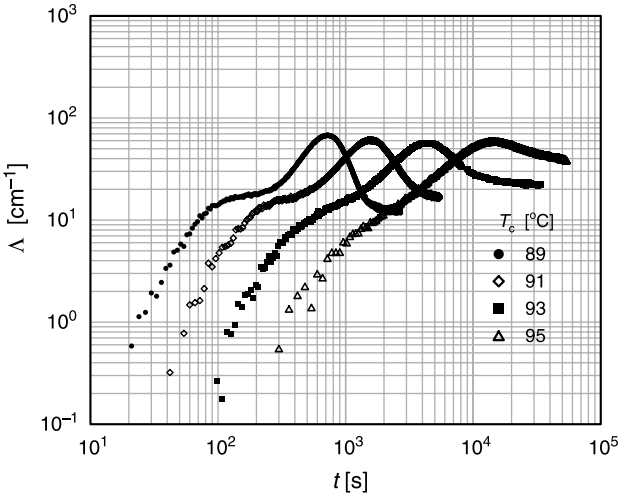


Fig. 8. P(PcoO14)D2: time dependence of the linear attenuation coefficient $\Lambda$ during isothermal crystallizations at the given temperatures. A crystallization in two steps is indicated.

Here $O_{ac}$ gives the crystalline–amorphous interface area per unit volume and $\Delta\eta_{ac}$ describes the electron density difference between the crystallites and the melt. For linearly growing spherulites with a constant inner structure one expects

$$P \sim t^3. \tag{26}$$

Fig. 7 shows that this is indeed found.

It is interesting to compare the time range covered by the attenuation measurements with that probed by dilatometry or SAXS. One can refer to the characteristic time at which the final plateau value is reached and consider the ratio of this final time to the beginning time where the first deviations from the melt values were detected. As the comparison shows, this 'dynamic range' is always larger for the attenuation measurement, even if the device in use has not yet been optimized.

The second investigated poly(ethylene-*co*-octene) sample, P(EcO14)D2, shows peculiarities in its crystallization behavior. Fig. 8 depicts the time dependence of $\Lambda$. Crystallization proceeds in this sample in two subsequent steps. A corresponding signal was found in the DSC curve. Cooling a sample from the melt also showed heat releases in two subsequent steps, which is shown in Fig. 9. Searching for the reason of this behavior, we found a difference in the crystallization properties of the core and the shell region of the supplied granular particles. Fig. 10 depicts the cooling curves obtained for material in the core and the shell region, respectively. The core region shows only one peak, that at the higher temperature, and the shell region is dominated by the second peak at lower temperatures. Interesting to note, both samples were annealed for 20 min at 160 °C, which is 30 K above the equilibrium melting point of the sample. In spite of that, the difference in the crystallization behavior between the two regions in the granular particles was not removed. This was achieved only by an annealing at even higher temperatures (180 °C) for even longer times (several hours).

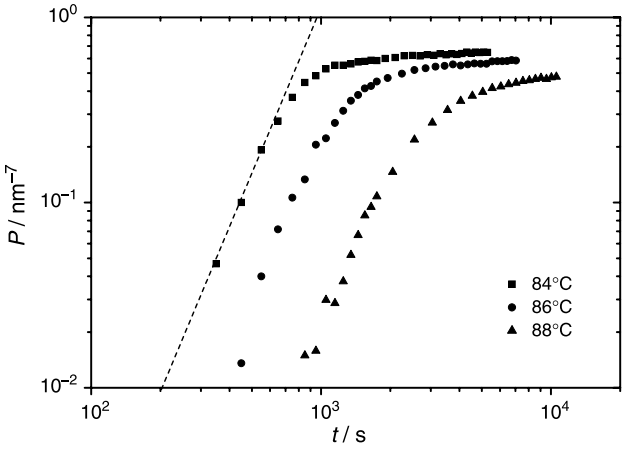


Fig. 7. P(PcoO14)D1, time-dependent SAXS: change of the Porod coefficient during isothermal crystallizations at the indicated temperatures. Slopes of the log–log plots indicate an initial increase proportional to $t^3$.

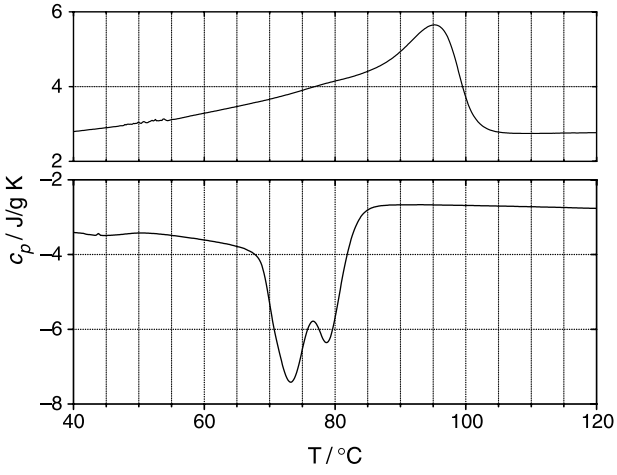


Fig. 9. P(PcoO14)D2: DSC thermograms obtained during a cooling–heating cycle with a cooling/heating rate of 10 K min$^{-1}$.

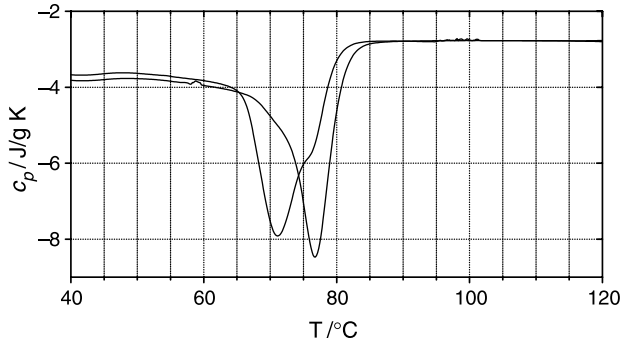


Fig. 10. P(PcoO14)D2, core and shell region of a granular particle: DSC thermograms obtained during cooling from the melt (cooling rate: 10 K $min^{-1}$).

## Acknowledgements

We highly appreciate the advice which we obtained from Georg Maret (University Konstanz). Funding of this work by the Deutsche Forschungsgemeinschaft is gratefully acknowledged. Thanks are also due to the 'Fonds der Chemischen Industrie' for financial support.

## References

[1] Imai M, Kaji K, Kanaya T, Sakai Y. Phys. Rev. B 1995;52:12696.
[2] Olmsted PD, Poon WCK, McLeish TCB, Terrill TCB, Ryan AJ. Phys. Rev. Lett. 1998;81:373–6.
[3] Kraak H, Deutsch M, Sirota EB. Macromolecules 2000;33:6174.
[4] Strobl G. Eur. Phys. J. E 2000;3:165.
[5] Kawai T, Strobl G. Macromolecules 2004;37:2249.
[6] Hawkins SW, Richards RB. J. Polym. Sci. 1949;4:515.
[7] Keane JJ, Stein RS. J. Polym. Sci. 1956;20:327.
[8] Levy B. J. Appl. Polym. Sci. 1961;5:408.
[9] Mahen KG, James WJ, Bosch W. J. Appl. Polym. Sci. 1965;9:3605.
[10] Kerker M. The Scattering of Light. New York: Academic Press; 1969 p. 37.
[11] Kerker M. The Scattering of Light. New York: Academic Press; 1969 p. 418.
[12] Meeten GH. Optical Properties of Polymers. Amsterdam: Elsevier; 1986.
[13] Schmidtke J, Strobl G, Thurn-Albrecht T. Macromolecules 1997;30:5804.
[14] Heck B, Strobl G. Colloid Polym. Sci. 2004;282:5117.
[15] Strobl G. The Physics of Polymers. Berlin: Springer; 1997 p. 184.